RADIAL TRANSPORT OF HIGH-ENERGY IONS CAUSED BY LOW-FREQUENCY FLUCTUATIONS IN THE GAMMA10 TANDEM MIRROR

M. Ichimura, Y. Yamaguchi, R. Ikezoe, Y. Imai, T. Murakami, T. Iwai,
T. Yokoyama, T. Sato, Y. Ugajin and T. Imai

Affiliation Information: Plasma Research Center, University of Tsukuba, 305-8577 Tsukuba, Japan
ichimura@prc.tsukuba.ac.jp

Plasmas with high ion-temperature of several keV have been produced by using ion-cyclotron range of frequency (ICRF) heating in the GAMMA 10 tandem mirror. In such high performance plasmas, high and low-frequency fluctuations are excited and ions trapped in the magnetic field interact with such fluctuations. Three types of wave-particle interactions have been observed in the GAMMA 10 tandem mirror. The turning point diffusion near the ion cyclotron resonance layer has been observed in minimum-B configuration on the anchor cell. Pitch angle scattering of high-energy ions due to the AIC modes and low-frequency waves which have differential frequencies between discrete peaks of the AIC modes are clearly detected. The drift-type fluctuations are clearly observed in the central cell. By using a semiconductor detector, high-energy ions are detected at the radial location far from the plasma edge. The fluctuation, of which frequency is the same as that of drift-type fluctuation, is observed in the signal of high-energy ions. From the pitch angle distribution of the phase differences between both fluctuations, radial transport of high-energy ions caused by drift-type fluctuations near their turning points in the confining mirror field is suggested in the experiments.

I. INTRODUCTION

Plasmas with ion temperature of several keV are produced and sustained stably by ion cyclotron range of frequency (ICRF) waves in the GAMMA 10 tandem mirror. Typical plasma parameters on axis in the central cell are density of 2×10^{18} m^{-3} and ion temperature of 5 keV. Saturation and/or the reduction of plasma parameters have been sometimes observed in high-power ICRF heating experiments. High-frequency fluctuations, so-called Alfvén-Ion-Cyclotron (AIC) waves[1], are spontaneously excited due to strong temperature anisotropy[2]. Low-frequency fluctuations are also observed in relation to applied ICRF powers and the amount of injecting gas. Two types of low-frequency fluctuations are identified; one is a flute-type fluctuation and the other is a drift-type fluctuation. The flute-type fluctuation is driven by the strong ion heating with fundamental ion-cyclotron resonances in the central cell and/or E×B rotation due to potential formation with electron-cyclotron heating (ECH) in plug/barrier cells. The drift-type fluctuations are observed in the case of high-power ICRF experiments. Interactions of ions with such high and low-frequency waves are possible candidates for the particle transport in both directions along and across the magnetic field line. In this manuscript, three types of wave-particle interactions observed in GAMMA 10 are reviewed. The first is turning-point diffusion along the cyclotron resonance layer in the minimum-B anchor cell[3]. The second is pitch angle scattering of high energy ions by the AIC waves[4] and low-frequency waves resulted from AIC waves[5]. The third is radial transport of high energy ions caused by low frequency fluctuations. The anomalous transport caused by those fluctuations is the critical problem in magnetically confined plasmas.

II. GAMMA 10 DEVICE AND DIAGNOSTICS

II.A. GAMMA 10 Device

GAMMA 10 is a minimum-B anchored tandem mirror with axisymmetric plug/barrier cells at both ends. The central cell has an axisymmetric mirror field and is 5.6m in length with the magnetic field strength of 0.4T at the midplane. The mirror ratio of the central cell is 5. The segmented-limiter of which diameter is 0.36 m is set near the midplane. The plasma is produced by applying RF power (RF1) in combination with short-pulse gun-produced plasmas from both ends and hydrogen gas injections near RF-antennas. The plasma is also heated by applying RF power (RF2) with the fundamental ion-cyclotron resonance layer near midplane of the central

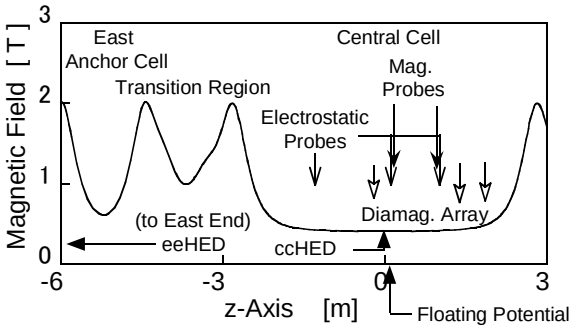

Fig. 1 Magnetic field profile in the axial direction and locations of diagnostics are indicated.

cell. In addition to the plasma production, RF1 is used for heating ions in minimum-B anchor cells[3]. The frequency of RF1 is selected to be a fundamental ion-cyclotron resonance frequency near the midplane of the anchor cell. Two types of antennas are installed in both ends (east and west) of the central cell. So-called Nagoya Type III antennas (driven by RF1) and conventional double half turn (DHT) antennas with single layer Faraday shield (driven by RF2) are used. Figure 1 shows the magnetic field profile and the locations of diagnostics for fluctuations and high-energy ions are shown in the figure. Figure 2 shows the temporal evolution of (a) ICRF pulse, (b) line density and (c) three diamagnetic signals at the different locations along the magnetic field in the typical

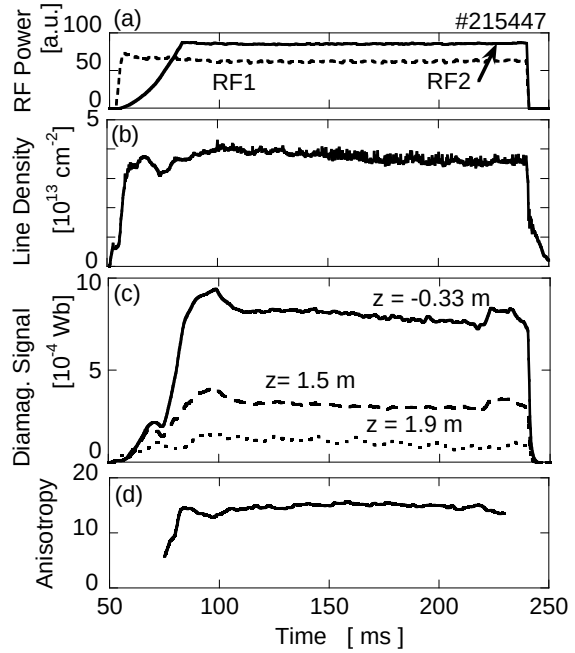

Fig.2. Temporal evolution of (a) ICRF pulse, (b) line density, (c) diamagnetic signals at z=-0.33 m, 1.5 m and 1.9 m, and (d) estimated pressure anisotropy

discharge. As shown in the figure, there are large differences between diamagnetic signals near the midplane (z = -0.33 m) and off-midplane (z = 1.5 m and z = 1.9 m). These differences indicate the pressure anisotropy. The pressure anisotropy in the axial direction is evaluated from these diamagnetic signals and indicated in Fig. 2(d). Plasmas with strong pressure anisotropy more than 10 are formed in the central cell. Alfvén-ion-cyclotron (AIC) modes are excited spontaneously due to such strong pressure anisotropy.

II.B. Fluctuation Measurements

Magnetic fluctuations excited in the plasma are measured by magnetic probe arrays both in the axial and azimuthal directions and density fluctuations are measured by electro-static probes (ESP) located in the axial and azimuthal directions as indicated in Fig. 1. A limiter located near the midplane is segmented in eight elements. Each element of the segmented-limiter is floated electrically from the ground. Then, the azimuthal distribution of the floating potential can be obtained. These low-frequency fluctuations are also observed in the floating potentials of each segment of the limiter.

II.C. High-Energy Ion Measurement

To measure high-energy ions, two semiconductor detectors are installed in GAMMA 10. One is an east-end high energy-ion detector, eeHED, of which configuration has been reported in Ref. 5. The other is a central-cell high energy-ion detector, ccHED, of which configuration is shown in Fig. 3. A silicon surface barrier (SSB) detector (nominal depletion depth of 300 μm) is used in this experiment. The sensitivity of the detector for protons has been indicated in Ref. 5. The ccHED has co-axial geometry and a fixed pin-hole aperture of which diameter is 0.5 mm is set in front of the SSB detector on an inner pipe. Pin-hole apertures of different diameters and an aperture covered with an aluminum foil of 2 μm thickness are set on the outer pipe. The outer pipe can rotate against to the inner pipe and can control the amount of input ion-flux and discriminate from electrons. The

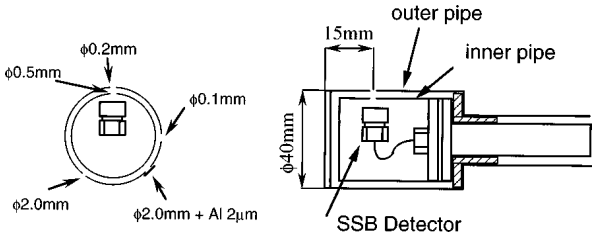

Fig. 3 Schematic drawing of ccHED which has co-axial configuration. Several apertures are set on the outer pipe.

ccHED is inserted perpendicularly to the magnetic field line and is located just outside of the limiter radius at the midplane of the central cell. Apertures are set in the direction from which ions enter with their diamagnetic motions. The detector does not look the plasma directly. By rotating the inner and outer pipes together, a pitch angle distribution of hot ions can be measured. When a minimum size aperture of which diameter is 0.2 mm is used, the pitch-angle resolution becomes ±3 degrees. When an aperture covered with aluminum foil is used, no signals are detected. When apertures are arranged in the electron diamagnetic direction, no signals are also detected. These experimental evidences imply the discrimination of protons from electrons, neutrals and UV.

III. EXPERIMENTAL RESULTS

III.A. Turning Point Diffusion near Cyclotron Resonance Layer [3]

In the standard magnetic field configuration of GAMMA 10, resonance layers for RF1 exist in both central and anchor cells. When the whole magnetic field strength is changed under a fixed RF1 frequency, an operation window of the magnetic field strength, in which plasmas can be sustained stably, appears. The enlarged magnetic field configuration near RF1 antenna and anchor midplane is indicated in Fig. 4. The contribution of each resonance layer to the plasma sustainment is confirmed by changing the magnetic field strength in the central and anchor cells independently. With a fixed magnetic field strength in the central cell, i.e. fixed conditions for the wave excitation by RF1, the plasma is sustained only in the range from B_A/B_{res} = 0.7 to 1.0, where B_A is the field strength of the anchor midplane and B_{res} is the resonant magnetic field strength for the applied RF1 frequency. The resonant field strength is indicated in Fig. 4 by a solid line of 0.63 T. A broken line labeled (a) is an upper limit

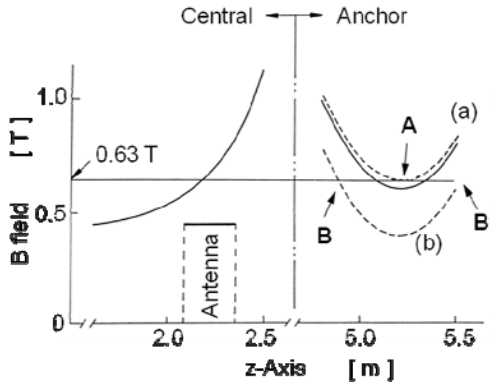

Fig. 4 Magnetic field configuration near the RF1 antenna and anchor midplane in the standard case (solid line). Upper limit (broken line A) and lower limit of the operation window (broken line B) are also indicated.

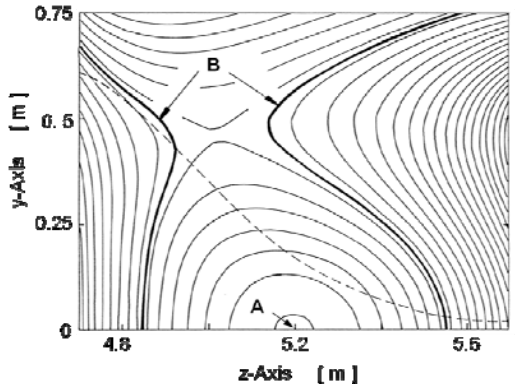

Fig. 5 Mod-B surfaces (solid lines) on the y-z plane in the anchor cell. The surface labeled **B** corresponds to the resonance layer in the case of broken line **B** of Fig.4.

of the field strength (B_A/B_{res} = 1.0), above which there are no resonance layers in the anchor cell. A broken line labeled (b) is a lower limit of the field strength (B_A/B_{res} = 0.7) for the plasma sustainment. Figure 5 shows the mod-B surface on y-z plane in the anchor cell. The upper limit corresponds to the boundary where the resonance layer disappears from the anchor midplane indicated by **A** in Figs. 4 and 5. It will be easy to understand the upper limit of the field strength is the limit of the cyclotron heating in the anchor cell. On the other hand, the lower limit of B_A/B_{res} = 0.70 corresponds to the boundary where the resonance layer is located on the mod-B surface which is not closed as indicated by label **B** in Fig. 5. The magnetic field is no longer minimum-B configuration from this surface. Since the turning point of the trapped ions has a tendency to center on the resonance layer, the guiding center of ions will drift on this surface because of the polarization drift caused by the RF field. In the minimum-B well, this surface is closed and the guiding center drift is restricted within the well. When this mod-B surface opens, ions can escape from the confinement region along the resonance layer.

III.B. Observation of Pitch Angle Scattering due to AIC-modes [4]

As described in Chapter II, the pressure anisotropy becomes greater than 10 and the AIC modes are spontaneously excited in the central cell with strong ICRF heating. The cyclotron resonance layers in this experiment are located at points of about 1 m from the midplane. Ions, of which turning point is the location of the cyclotron resonance layer, have their pitch angle of 80 degrees at the midplane. ccHED can measure the pitch angle distribution of hot ions and eeHED can measure the hot ions which are scattered into the loss cone of the central cell. There is a clear correlation between the

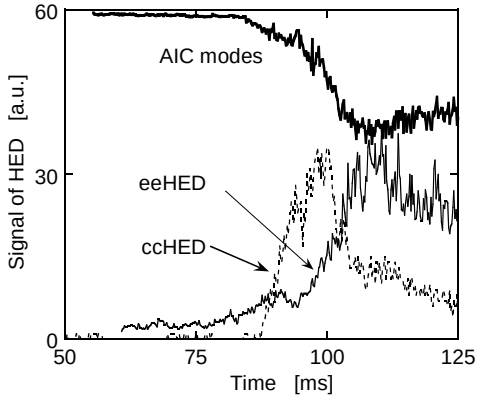

Fig. 6 Temporal evolution of ccHED and eeHED signals and the amplitude of the AIC-modes.

amplitude of the AIC-modes and signals of ccHED and eeHED. When the diamagnetic signal reaches a threshold value, the ccHED signal appears and abruptly increases with the diamagnetic signal because the SSB detector can detect only high energy ions. The ccHED signal increases with the diamagnetic signal on the initial phase and turns to decrease though the diamagnetic signal is still increasing. The AIC modes appear under the certain conditions of the anisotropy and the plasma beta. The eeHED signal increases as the AIC modes are excited. The temporal evolution of the end-loss high energy ions is almost the same as that of the AIC amplitude. When the amplitude of the AIC modes becomes strong, high energy

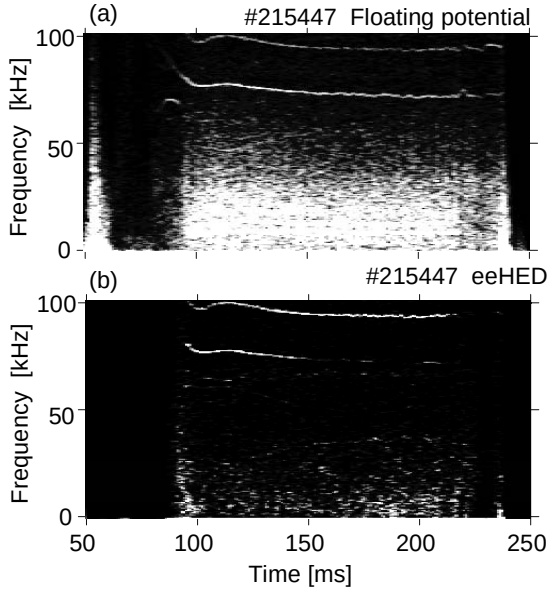

Fig. 7 Temporal evolution of intensity plots of frequency spectrum; (a) floating potential of the segmented-limiter and (b) high-energy ions to the east end (eeHED).

ions with a pitch angle near 90 degrees begin to decrease and eeHED signal increases. Figure 6 shows the temporal evolution of the ccHED and eeHED signals and the amplitude of the AIC-modes. This experimental observation indicates the pitch angle scattering of hot ions due to the AIC modes.

Recently, magnetic probes, of which cross section is larger than that of the conventional pick-up loops for measuring ICRF waves, have been installed to measure low-frequency magnetic fluctuations. Low-frequency magnetic fluctuations around 100 kHz, which are differential frequencies between each discrete peak of the AIC modes, are clearly detected. These fluctuations are also detected in the ion saturation current detected by ESP and floating potentials of the segmented-limiter near the midplane of the central cell. The density fluctuations will be induced due to the AIC modes. On the signals of the high-energy ions in eeHED, these fluctuations are also clearly observed. As reported in the following section, the radial transport of high-energy ions due to drift-type fluctuations is observed with ccHED in the central cell. Figure 7 shows the temporal evolution of intensity plots of frequency spectrum; (a) floating potential of the segmented-limiter and (b) high-energy ions to the east end (eeHED). In both signals, frequency peak around 80 kHz are clearly indicated. Strong signals in the frequency less than 20 kHz are only observed in the floating potential signal and are not observed in the eeHED signal. These low-frequency signals correspond to drift-type fluctuations. These experimental observations also indicate the pitch angle scattering due to the AIC modes.

III.C. Radial Transport Caused by Low-Frequency Fluctuations

III.C.1 Reconsideration of the ccHED signal

Before discussions about the radial transport caused by low-frequency fluctuations, the ccHED signal must be reconsidered for the interpretation of the experimental results. SSB detectors can measure the energy of incident particles from their pulse height as shown in Fig.8. For the calibration of the pulse height of the detector, α-

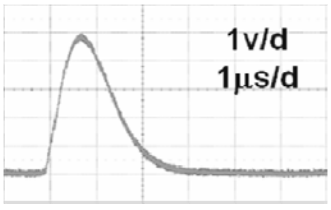

Fig. 8 Calibration signal of ccHED with an α-particle of which energy is 5.5 MeV from a radioisotope of Am-241. Pulse height is about 5 V and pulse width is near 2 μs at the present amplifier gain.

particles emitted from a radioisotope Am-241, of which energy is 5.5 MeV, are used. As shown in Fig.8, a pulse with the amplitude near 5 V and the width near 2 μsec is detected at the present amplifier gain.

When ccHED is set far from the plasma edge, periodic peaks are obtained discretely as shown in Fig.9. Figure 9 shows (a) whole ccHED signal, (b) expanded signal from 82 ms to 83 ms and (c) from 82.1 ms to 82.3 ms. At the location of 7 cm from the limiter radius, Larmor radius of 10 keV protons is 1.4 cm and ccHED is considered to be set far from the plasma edge. The pulse height reaches more than 10 V and the width is about 10 μs. Because the appearance of high energy ions more than 10 MeV is not realistic, each discrete peak is considered to contain several tens particles and is burst-like escaping high-energy ions. The period of these bursts corresponds to the frequency of the drift-type fluctuations observed in the ESP signal.

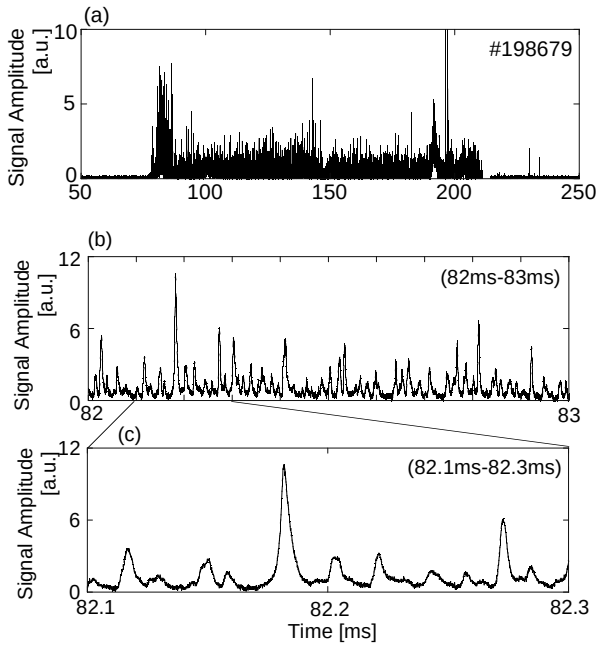

Fig. 9 ccHED signal at the location of 7 cm from the limiter radius. (a) whole signal, (b) expanded signal from 82 to 83 ms and (c) from 82.1 to 82.3 ms.

III.C.2 Fluctuations in the ccHED signal

Figure 10 shows intensity plots of the temporal evolution of the frequency spectrum; (a) ion saturation current measured by ESP and (b) high energy ions by ccHED. As mentioned previously, a drift-type fluctuation, of which frequency is near 8 kHz, is observed strongly from 100 ms to 150 ms. From 150 ms, the plasma is used for another experiment and we now focus to signals between 100 and 150 ms. Figure 10 (a) shows the density fluctuations measured near the midplane of the central cell (z = 0.33 m). In the axial direction, this fluctuation propagates and is detected at the plug/barrier cell (z = 7.7 m). In the azimuthal direction, this fluctuation has a mode number of m = +1, which means a rotation in the electron diamagnetic direction. Figure 10 (b) shows the frequency spectrum of high-energy ions with a pitch angle of 85 degrees. The spectrum is fairly noisy compared to that of the ESP signal, however, a clear peak with the same frequency as that in the ESP signal is still identified. The significant reduction of the diamagnetism is sometimes observed when the amplitude of the fluctuations increases. In such an unstable discharge, it has been clearly observed that the ccHED signal increases and the eeHED signal decreases[6]. These experimental observations will indicate the radial transport of high-energy ions caused by the drift-type fluctuations. The high-energy ions are detected at the location far from the limiter radius with the frequency of the drift-type fluctuations.

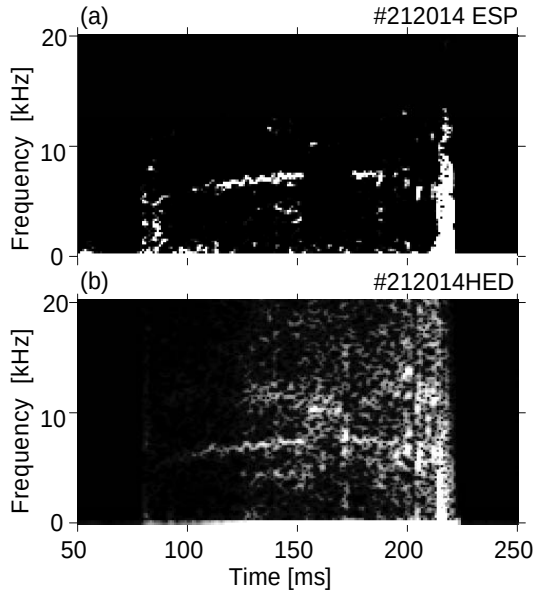

Fig. 10 Intensity plots of the temporal evolution of the frequency spectrum; (a) ion saturation current measured by ESP and (b) high energy ions by ccHED.

III.C.3 Pitch angle dependence of phase differences between fluctuations in the ESP signal and the ccHED signal

As described in previous section, ccHED can measure the pitch angle distribution of high-energy ions at the midplane. The pitch angle of ions confined in the magnetic mirror configuration is equivalent to their turning points. It will be considered that ions interact with waves mainly near their turning points due to long interaction time. To clarify the radial transport of high-

energy ions caused by low-frequency fluctuations, the pitch angle dependence of the interaction between fluctuations and high-energy ions is analyzed. Figure 11 shows the phase differences between the density fluctuations measured by ESP and the fluctuations of high-energy ions measured by ccHED in the cases of the pitch angle 85, 75 and 65 degrees. The pitch angle dependence is clearly shown in the figure. It is difficult to determine the absolute phase difference between both signals. When the pitch angle is 90 degrees, the phase difference can be defined as zero because ccHED is located just at the midplane of the central cell. At present, the resolution of the pitch angle is not so small and phase differences plotted in Fig. 11 are fairly scattered. Averaged phase differences in cases of ions with pitch angles 85, 75 and 65 degrees are 1.62, 0.91 and 0.54 radians, respectively. Then, the difference of the ccHED signal of 65 degrees from that of 85 degrees becomes about 1.08 radians. The distance between turning points of ions with pitch angles of 65 and 85 degrees is about 1.2 m, which is calculated from the magnetic field profile, shown in Fig. 1. The axial wave number of the fluctuation is about 1.1 m^{-1} in this experiment, which is estimated from two ESPs arrayed in the axial direction. Then, the phase difference of the fluctuation in cases of ions with pitch angles 65 and 85 degrees becomes 1.3 radians. This value is almost same value as the phase difference obtained from the ccHED signals. It will be possible to consider that hot ions interact with those fluctuations near the turning points.

IV. SUMMARY

Three types of wave-particle interactions observed in GAMMA 10 are reviewed. The first is the turning point diffusion near the cyclotron resonance layer in minimum-B configuration on the anchor cell. The second is the pitch angle scattering of high-energy ions due to the AIC modes and low-frequency waves which have differential frequencies between discrete peaks of the AIC modes. The third is the radial transport of high-energy ions caused by drift-type fluctuations near their turning points in the confining mirror field.

ACKNOWLEDGMENTS

The authors acknowledge the GAMMA 10 group at the University of Tsukuba for their collaboration. This work is partly supported by Grant-in-Aid for Scientific Research under the Ministry of Education, Culture, Sports, Science and Technology, Japan (No.21540506) and also partly supported by the bidirectional collaborative research program of National Institute for Fusion Science, Japan (NIFS09KUGM040).

REFERENCES

1. G.SMITH, *Phys. Fluids*, **27**, 1499 (1984).
2. M.ICHIMURA, et al., *Phys. Rev. Lett.*, **70**, 2734 (1993).
3. M.ICHIMURA, et al., *Nuclear Fusion*, **28,** 799 (1988)**.**
4. M.ICHIMURA, et al., *Nuclear Fusion*, **39**, 1707 (1999).
5. T.SAITO, et al., *Rev. Sci. Instrum.*, **68**, 1433 (1997)
6. M.KATANO, et al., *Trans. of Fusion Sci. and Tech.*, **51** 289 (2007).

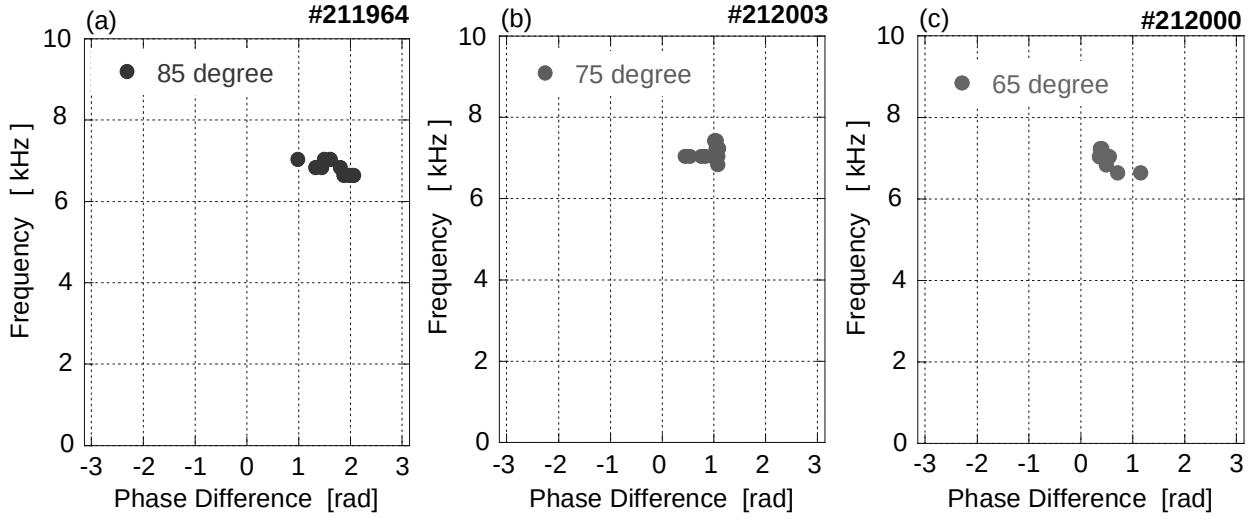

Fig. 11 Phase differences between the density fluctuations measured by ESP and the fluctuations of high-energy ions measured by ccHED in the cases of the pitch angle (a) 85, (b) 75 and (c) 65 degrees.